ORIGINAL ARTICLES

WILEY

Synchronization of repolarization after cardiac resynchronization therapy: A combined clinical and modeling study

Nienke J. Verzaal PhD[1] | Caroline J. M. van Deursen MD, PhD[2] |
Simone Pezzuto PhD[3] 🄳 | Liliane Wecke MD, PhD[4] |
Wouter M. van Everdingen MD, PhD[5] | Kevin Vernooy MD, PhD[2] |
Tammo Delhaas MD, PhD[6] | Angelo Auricchio MD, PhD[3,7] | Frits W. Prinzen PhD[1] 🄳

[1]Department of Physiology, Cardiovascular Research Institute Maastricht, Maastricht University, Maastricht, The Netherlands

[2]Department of Cardiology, Maastricht University Medical Center, Maastricht, The Netherlands

[3]Center for Computational Medicine in Cardiology, Euler Institute, Università della Svizzera italiana, Lugano, Switzerland

[4]Heart Clinic, Capio St. Göran's Hospital, Sankt Göransplan 1, Stockholm, Sweden

[5]Department of Radiology and Nuclear Medicine, Radboudumc, Nijmegen, The Netherlands

[6]Department of Biomedical Engineering, Maastricht University, Maastricht, The Netherlands

[7]Department of Cardiology, Istituto Cardiocentro Ticino, Lugano, Switzerland

Correspondence

Frits W. Prinzen, PhD, Department of Physiology, Cardiovascular Research Institute Maastricht, Maastricht University, P.O. Box 616, 6200 MD Maastricht, The Netherlands.
Email: frits.prinzen@maastrichtuniversity.nl

Abstract

Introduction: The changes in ventricular repolarization after cardiac resynchronization therapy (CRT) are poorly understood. This knowledge gap is addressed using a multimodality approach including electrocardiographic and echocardiographic measurements in patients and using patient-specific computational modeling.

Methods: In 33 patients electrocardiographic and echocardiographic measurements were performed before and at various intervals after CRT, both during CRT-ON and temporary CRT-OFF. T-wave area was calculated from vectorcardiograms, and reconstructed from the 12-lead electrocardiography (ECG). Computer simulations were performed using a patient-specific eikonal model of cardiac activation with spatially varying action potential duration (APD) and repolarization rate, fit to a patient's ECG.

Results: During CRT-ON T-wave area diminished within a day and remained stable thereafter, whereas QT-interval did not change significantly. During CRT-OFF T-wave area doubled within 5 days of CRT, while QT-interval and peak-to-end T-wave interval hardly changed. Left ventricular (LV) ejection fraction only increased significantly increased after 1 month of CRT. Computer simulations indicated that the increase in T-wave area during CRT-OFF can be explained by changes in APD following chronic CRT that are opposite to the change in CRT-induced activation time. These APD changes were associated with a reduction in LV dispersion in repolarization during chronic CRT.

Conclusion: T-wave area during CRT-OFF is a sensitive marker for adaptations in ventricular repolarization during chronic CRT that may include a reduction in LV dispersion of repolarization.

KEYWORDS

cardiac resynchronization therapy, computer modeling, heart failure, repolarization, vectorcardiography

1 | INTRODUCTION

Cardiac resynchronization therapy (CRT) is a nonpharmacological therapy recommended by clinical practice guidelines in heart failure patients with reduced left ventricular (LV) ejection fraction and QRS duration >130 ms.[1] CRT significantly reduces mortality and heart failure hospitalizations. This beneficial effect is clearly linked to resynchronization of electrical activation, recoordination of contraction, and accompanying improvement in pump function and cardiac reserve.

Electrocardiographic changes of depolarization after CRT have been studied in considerable detail; in contrast, less is known about changes in repolarization caused by CRT. A few studies in both animal tissues and humans reported increased dispersion of repolarization during CRT, possibly suggesting an increased risk for ventricular arrhythmias.[2,3] On the other hand, large clinical trials and multiple registries showed a significantly lower risk of ventricular tachycardia or ventricular fibrillation in CRT patients, in particular in those patients who show significant reverse remodeling.[4–6] These clinical observations suggest that adaptations in ventricular repolarization may occur after CRT. However, little is known about longitudinal changes of ventricular repolarization and their relation to reverse remodeling induced by CRT.

To address this gap in evidence, a multimodality approach including electrocardiography (ECG), vectorcardiography (VCG), and echocardiography, supplemented by patient-specific modeling was considered. In the present study, we investigated in a cohort of consecutive CRT patients: (1) the time course and extent of changes in T-wave markers recorded using sequential 12-lead ECGs in patients after the start of CRT; (2) the potential mechanisms behind these T-wave changes using a personalized computer model of activation and repolarization.

2 | MATERIALS AND METHODS

2.1 | Patients

Patients who were referred to Maastricht University Medical Centre between March 2010 and May 2012, who were 18 years of age or older; had an indication for CRT; did not have any known condition that could limit life expectancy to less than 6 months as of referral; and were capable of giving informed consent were asked to participate. In this publication only data are included of a subgroup of 33 patients who agreed to frequently return to the hospital to record ECGs and echocardiograms at several time points after CRT implant. The study conforms to the Declaration of Helsinki. The protocol was approved by the ethics committee of Maastricht University Medical Centre (project number 10-2-090). All patients gave written informed consent before inclusion.

2.2 | Study protocol

The 12-lead ECG was obtained before and 1 day, 5 days, 2 weeks, and 1, 3, and 6 months after implantation. Echocardiography was performed 3 months to 1 day before and 1 and 14 days as well as 6 months after implantation. Postimplant ECG and echocardiographic measurements were obtained with both CRT-ON and while the CRT device was briefly switched off (CRT-OFF).

2.3 | VCG analysis

ECGs were extracted from the MUSE Cardiology Information system (GE Healthcare). Using custom-written Matlab software, ECGs were transformed to VCGs utilizing the Kors matrix and semi-automatic analysis was performed.[7] Amplitude of the QRS and T vectors were defined as the maximum distances between the origin of the VCG loop and a point on the 3D QRS and T loops, respectively. The area under the curve of the QRS and T-wave in the X, Y, and Z direction was determined by numerical integration from the beginning to the end of the QRS complex or T-wave, respectively. Subsequently, the total area of the QRS and T loops were determined using the equations:

$$QRS_{area} = \sqrt{QRS_{area,x}^2 + QRS_{area,y}^2 + QRS_{area,z}^2}$$

and

$$T_{area} = \sqrt{T_{area,x}^2 + T_{area,y}^2 + T_{area,z}^2},$$

subscripts x, y, and z denoting the three orthogonal VCG leads.

QT interval was measured automatically using the tangent method[8] and subsequently corrected for heart rate (QT-corrected [QTc]) using Fridericia's formula.[9] Median T peak-to-end interval

(Tp-e) as well as precordial QT dispersion (standard deviation of start Q to precordial T ends) of all leads were determined.

2.4 | Echocardiography

Echocardiograms were obtained using an iE33 system (Philips Medical Systems). Left ventricular end-systolic volume (LVESV) and ejection fraction (LVEF) were calculated using the biplane (modified Simpson's rule) or monoplane method in the apical four-chamber window if the apical two-chamber view was of insufficient quality. Mean values from three consecutive beats are reported. CRT response was defined as a reduction of LVESV ≥ 15% or an absolute increase of LVEF ≥ 5%, after 6-months CRT.

Using speckle tracking analysis (QLAB version 8.1; Philips Medical Systems) septal strain was determined on apical four chamber views, focussed on the interventricular septum. These focussed views of the interventricular wall are most optimal for showing paradoxical motion before CRT.[10] Systolic rebound stretch of the septum (SRSsept), a strong indicator of CRT response, was defined as the total amount of stretch during systole that occurred after initial shortening.[11]

2.5 | In silico modeling

Patient-specific computer simulations were performed with an eikonal model of cardiac activation and surface ECG.[12] The model determines the activation times (ATs) starting from patient-specific earliest activation sites (EASs) and conduction velocity (CV). The repolarization times (RTs) are obtained as the sum of AT and patient-specific action potential duration (APD). The ECG was computed using the lead field theory[13] and a template-based transmembrane potential in the myocardium as follows:

$$V_m(x, t) = V_0 + \frac{V_1 - V_0}{2}\left(\tanh\left(\frac{t - AT(x)}{\epsilon_0}\right) - \tanh\left(\frac{t - RT(x)}{\epsilon_1(x)}\right)\right),$$

where $V_0 = -85mV$, $V_1 = 30mV$, and $\epsilon_0 = 1ms$.

In this study, we considered a single anatomical model from a patient with no history of scar, who was participating in an earlier study performed at the Center for Computational Modeling in Cardiology (Università della Svizzera italiana, Lugano, Switzerland).[14] cardiac magnetic resonance (CMR) data were used to construct the heart-torso model, comprising ventricles with valve plane and outflow tracts, atrial blood cavities, aorta and major vessels, lungs, torso, and electrodes position. Patient ECG was used to fit the baseline computer model, by iteratively adjusting the parameters (EASs, CV, APD, and ϵ_1) until differences between measured and simulated ECG were minimal in the least-squares sense.[14] CV, APD, and repolarization rate ϵ_1 were adjusted in six myocardial compartments: LV and RV endocardium, mid-myocardium, and epicardium. Mid-myocardium and epicardium respectively covered 30% and 20% of the transmural thickness.

Acute CRT was simulated by biventricular pacing, with manually placed leads on LV epicardium and RV apex and no interventricular delay. Changes in RT during chronic CRT was modeled by locally decreasing the APD proportionally to the difference between depolarization time after and prior CRT: $RT^{chronic} = RT^{base} - x \cdot (AT^{CRT} - AT^{base})$. The factor x was varied between 0.5 and 0.8 to find the best match with the measured T-wave parameters. The ECGs of four scenarios (baseline, acute CRT-ON, chronic CRT-ON, and chronic CRT-OFF) were analyzed with the same workflow adopted for the clinical cohort (see above). Simulated baseline T-wave area value was multiplied by a normalization factor to match the average baseline T-wave area value in the patient cohort. All other simulated T-wave and QRS area values were multiplied by the same factor. APD90 was defined as the time at which the action potential reached 90% of its resting potential during the repolarization phase.

TABLE 1 Patient characteristics

Age (years)	67 ± 8
Female (n, %)	10 (30)
BMI (kg/m^2)	27 ± 5
NYHA class	
I (n, %)	6 (18)
II (n, %)	12 (36)
III (n, %)	12 (36)
IV (n, %)	3 (9)
Ischemic cardiomyopathy (n, %)	19 (58)
AF (n, %)	8 (24)
LBBB (n, %)	28 (85)
Previous RV pacing (n, %)	4 (12)
ACE-inhibitor/ARB (n, %)	30 (91)
Beta blocker (n, %)	31 (94)
Aldosterone antagonist (n, %)	8 (24)
Loop diuretic (n, %)	21 (64)
CRT responders (n,%)	18 (60)
Biventricular pacing (%, median [IQR])	98.8 (97.4–99.4)
LV lead location (n,%)	
Basal inferolateral	1 (3)
Basal anterolateral	9 (27)
Mid inferior	2 (6)
Mid inferolateral	8 (24)
Mid anterolateral	10 (30)
Apical lateral	3 (9)

Note: Variables are shown as mean ± SD or as number of patients (percentage of patients).

Abbreviations: ACE, angiotensin converting enzyme; AF, atrial fibrillation; ARB, angiotensin receptor blocker; CRT, cardiac resynchronization therapy; IQR, interquartile range; LBBB, left bundle branch block; LV, left ventricular; RV, right ventricular.
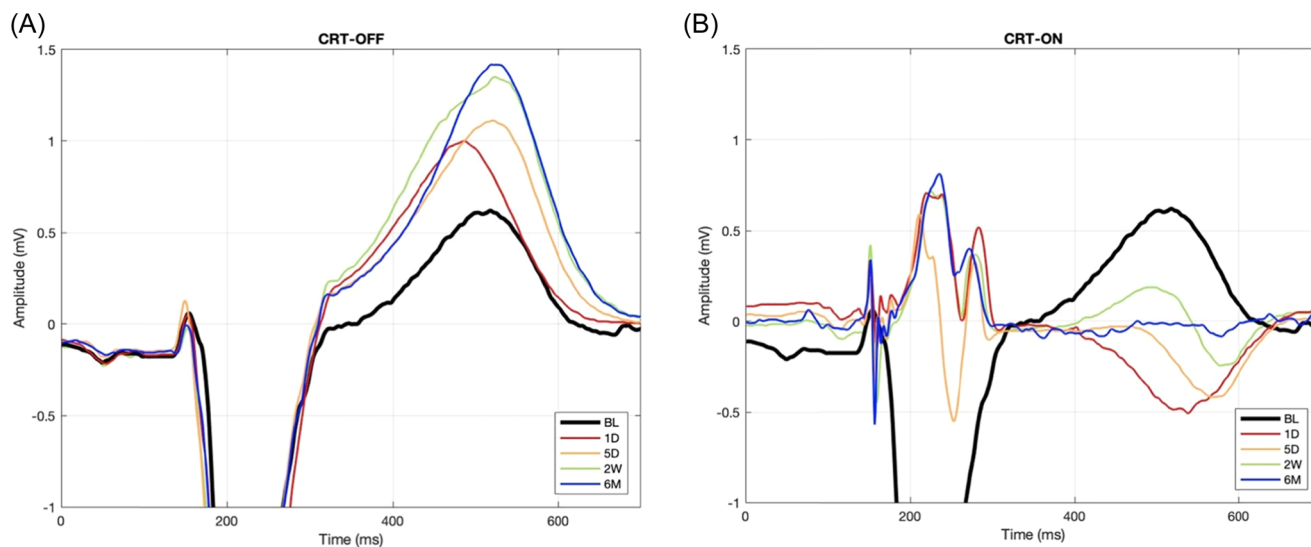
FIGURE 1 Example ECGs (lead V2) of a patient during CRT-OFF (A) and CRT-ON (B). CRT, cardiac resynchronization therapy; ECG, electrocardiography.

2.6 | Statistical analysis

All analyses were carried out in GraphPad Prism 8 (GraphPad Software). Analysis was performed either by fitting a mixed model, a one-way repeated measures analysis of variance (ANOVA) or two-way mixed effects ANOVA, as appropriate, followed by a Bonferroni's multiple comparisons test. We applied the Geisser-Greenhouse correction during ANOVA to account for possible violations of the assumption of sphericity. Parameters with only baseline and one follow-up value (e.g., LVEF) were assessed using a paired t-test. For comparison of continuous variables between subgroups, an unpaired t-test was employed. Categorical variables were compared using Fisher's exact test, except for LV lead locations, due to low patient numbers in multiple categories. For NYHA class comparison between the two subgroups, classes I & II and III & IV were combined to increase the number of patients per category. Two-sided p-values ≤.05 were considered statistically significant. Data are shown as mean ± SD or median (interquartile range).

3 | RESULTS

Baseline characteristics of the cohort are presented in Table 1 and show a typical population of CRT patients.

3.1 | Electrical and echocardiographic parameters over time

Figure 1 shows examples of ECG lead V2 of a patient during both CRT-OFF (A) and CRT-ON (B) at various time points. CRT-ON caused immediate amplitude reduction and narrowing of the QRS complex, as well as reduction in QRS area (Figure 2A, Table 2), indicating resynchronization of activation. Although Figure 1 shows

considerable changes in the T-wave during CRT-ON and CRT-OFF, changes in two conventional indicators of repolarization (QTc and Tp-e) were insignificant during CRT-ON and only moderately increased during CRT-OFF (Figure 2C,D, Table 2). In contrast, T-wave area and amplitude decreased by approximately 40% during CRT-ON while almost doubling during CRT-OFF (both $p < .05$). Notable was that the values of T area reached the plateau after approximately 5 days (Figure 2B).

Of the echocardiographic measures, SRSsept decreased immediately upon start of CRT (Figure 2E), but it took approximately 2 weeks before LVEF started to increase (Figure 2F). LVEF remained unchanged after temporarily halting CRT, in contrast to SRSsept (CRT-OFF, Figure 2E,F). Sixty percent of patients were echocardiographic CRT responders.

3.2 | In silico results

Figure 3A displays the patient-specific heart-torso model, derived from CMR measurements. Figure 3B displays the AP morphologies at baseline, indicating that the optimal match between measured and simulated ECG coincided with shorter APs in the RV than in the LV and with a more triangular AP shape in the RV and LV epicardium and RV endocardium than in the other layers. Figure 3C,D shows the recorded baseline ECG as well as the simulated baseline and follow-up ECG (lead V2) during CRT-ON and CRT-OFF.

To obtain the best fit of simulated and measured baseline ECG of the patient, the patient-specific activation model included four EASs along the RV endocardium (two basal-septal and two RV free wall, Figure 4A, TOP panel), thus indicating a left bundle branch block (LBBB)-like depolarization sequence. Simulated and recorded baseline ECG of the patient correlated very well (Pearson's correlation $r = .96$). Simulated ECGs at the four time points also closely
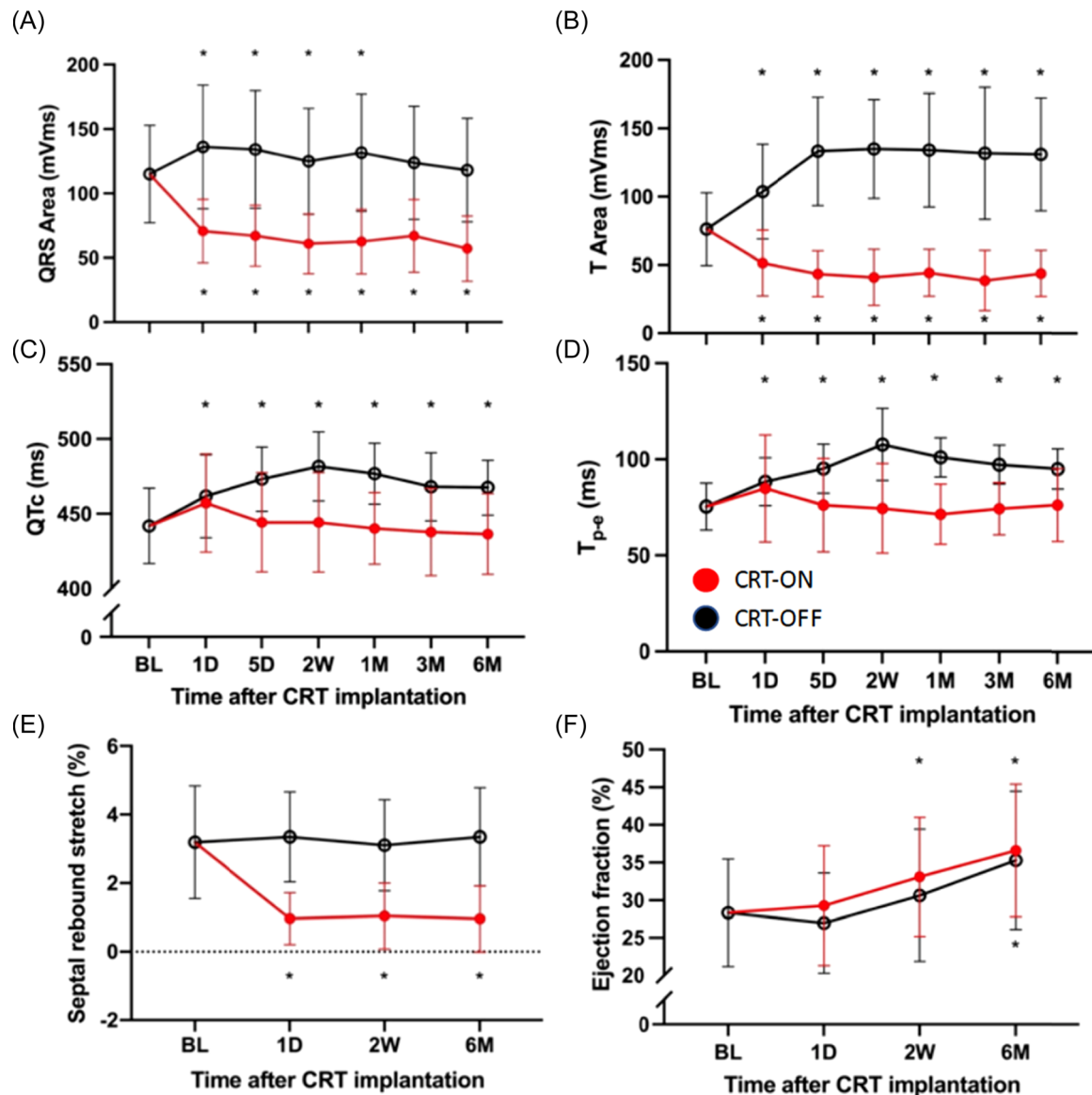
FIGURE 2 Electrocardiographic and echocardiographic parameters during CRT-OFF (black symbols) and CRT-ON (red symbols). (A) QRS area. (B) T area. (C) QTc interval. (D) T_{p-e}. (E) Septal rebound stretch. (F) Ejection fraction. *$p \leq .05$ versus BL. 1D, 1 day; 5D, 5 days; 2W, 2 weeks; 1M, 1 month; 3M, 3 months; 6M, 6 months; BL, baseline; CRT, cardiac resynchronization therapy.

resembled the measured ones presented in Figure 1, both showing an increase in T-wave size over time during CRT-OFF (Figure 3C) and a partial return of the T-wave polarity toward baseline during chronic CRT-ON (Figure 3D).

The depolarization and repolarization maps during acute CRT (Figure 4, second row, obtained using the baseline APD distribution), showed resynchronization of depolarization and, to some extent, also repolarization.

The best match between the measured and simulated relative increase in T-wave area was achieved by assuming that APD during chronic CRT changed according to an inverse relation between the CRT-induced change in AT and change in APD with a slope of 0.6 (see Section 2; Figure 3). The model also recapitulated the minor changes in QT time. The adaptation in APD resulted in an increase in APD in the LV

lateral wall and a reduction in RV APD (Figure 4B,C, middle two panels), coinciding with an increase in overall dispersion of APD. During chronic CRT-OFF, so returning to the LBBB-like activation pattern, the adaptation-induced distribution of APD resulted in considerably delayed repolarization in the LV free wall (Figure 4, bottom row), which was associated with an increase in T-wave area derived from the patient-specific simulation (from 76 to 139 mV·ms).

The finite difference model allowed to calculate both RV and LV dispersion of repolarisation in all 350 000 computational vertices, with a spatial resolution of 1 mm (Figure 5). At baseline, overall RV repolarization preceded that of the LV. Acute CRT led to reduction of interventricular differences in RT, but mean RV repolarization preceded that of the LV again after chronic CRT. Acute CRT reduced LV repolarization dispersion, but increased RV repolarization dispersion. After chronic CRT RV

	BL	1D	5D	2W	6M
Heart rate (bpm)					
OFF	69 ± 9	67 ± 13	66 ± 10	65 ± 10	61 ± 7*
ON		68 ± 10	67 ± 8	68 ± 9	65 ± 10
QRS duration (ms)					
OFF	187 ± 17	189 ± 17	185 ± 14	185 ± 22	179 ± 17
ON		156 ± 18*	151 ± 17*	151 ± 20*	157 ± 24*
QRS amplitude (mV)					
OFF	1.5 ± 0.4	1.8 ± 0.5*	1.8 ± 0.5*	1.7 ± 0.5*	1.7 ± 0.5*
ON		1.2 ± 0.4*	1.2 ± 0.4*	1.1 ± 0.3*	1 ± 0.3*
T amplitude (mV)					
OFF	0.5 ± 0.2	0.6 ± 0.2	0.8 ± 0.2*	0.8 ± 0.2*	0.8 ± 0.2*
ON		0.4 ± 0.2*	0.3 ± 0.1*	0.3 ± 0.1*	0.3 ± 0.1*
QRS/T area ratio					
OFF	1.5 ± 0.3	1.3 ± 0.2*	1 ± 0.1*	0.9 ± 0.2*	0.9 ± 0.1*
ON		1.6 ± 0.8	1.7 ± 0.7	1.7 ± 0.9	1.5 ± 1.1

TABLE 2 Values of electrical variables at several time points during CRT (ON) and when temporarily interrupting CRT (OFF), shown as mean ± SD

Abbreviations: 1D, 1 day; 5D, 5 days; 2W, 2 weeks; 1M, 1 month; 3M, 3 months; 6M, 6 months; BL, baseline; CRT, cardiac resynchronization therapy.

*$p \leq .05$ versus BL.

dispersion returned to almost baseline values while LV dispersion further decreased. Turning CRT off increased both inter- and intraventricular repolazation dispersion to values above baseline. The black arrows, representing the last ventricular repolarization, indicate that acute CRT slightly prolongs the time of last repolarization, that this time becomes shorter between acute and chronic CRT-ON, and prolongs considerably when returning from chronic CRT-ON to CRT-OFF, resembling the changes observed in QTc (Figure 2C).

4 | DISCUSSION

The main findings of this study are that (1) T-wave area during transient halting of CRT (CRT-OFF) seems to be a more sensitive marker for adaptations in ventricular repolarization than conventional measures such as QTc and Tp-e; (2) T-wave area changes reach a plateau within a week of CRT, preceding the increase in LVEF; and that 3) patient-specific computer simulations indicate that these T-wave changes may be explained by an inverse relation between changes in AT and APD that coincide with a reduction in RV and LV dispersion of repolarization during chronic CRT.

4.1 | T-wave changes following longer lasting CRT

The observed T-wave changes during CRT appear in line with previously described T-wave changes after development of LBBB or start of RV pacing. Under such conditions the T-wave increases immediately upon the change in activation sequence, while its size decreases during subsequent days to weeks,[14,15] a time span similar to that observed in our CRT study. However, during continuining CRT (with CRT-ON) the ~50% reduction in T-wave area over time occurred quickly, reaching a plateau phase within a day. In contrast, the T-wave area during CRT-OFF doubled, provided a stronger biological signal, while it took about a week to reach the plateau phase.

Such relatively slow T-wave changes during CRT-OFF are comparable to the phenomenon of cardiac memory, which is observed when returning to normal activation after a period of (single) ventricular pacing or ventricular conduction abnormality.[16] When pacing is switched off, the T-wave shape remains abnormal despite the return to the baseline QRS complex. In the context of CRT, interruption of pacing lets the heart return to the abnormally activated baseline state (i.e., LBBB), allowing comparison of the T-wave during CRT-OFF and baseline with a (major) difference in the QRS complex.

4.2 | Changes in APD

Studies have shown that the T-wave changes during cardiac memory occur due to regional changes in APD, that is, APD prolongation in early activated regions and APD shortening in regions of late activation during the dominant activation sequence.[17,18] The model simulations presented in this study indicate that this way of adaptation may also occur in CRT patients. Comparable differences
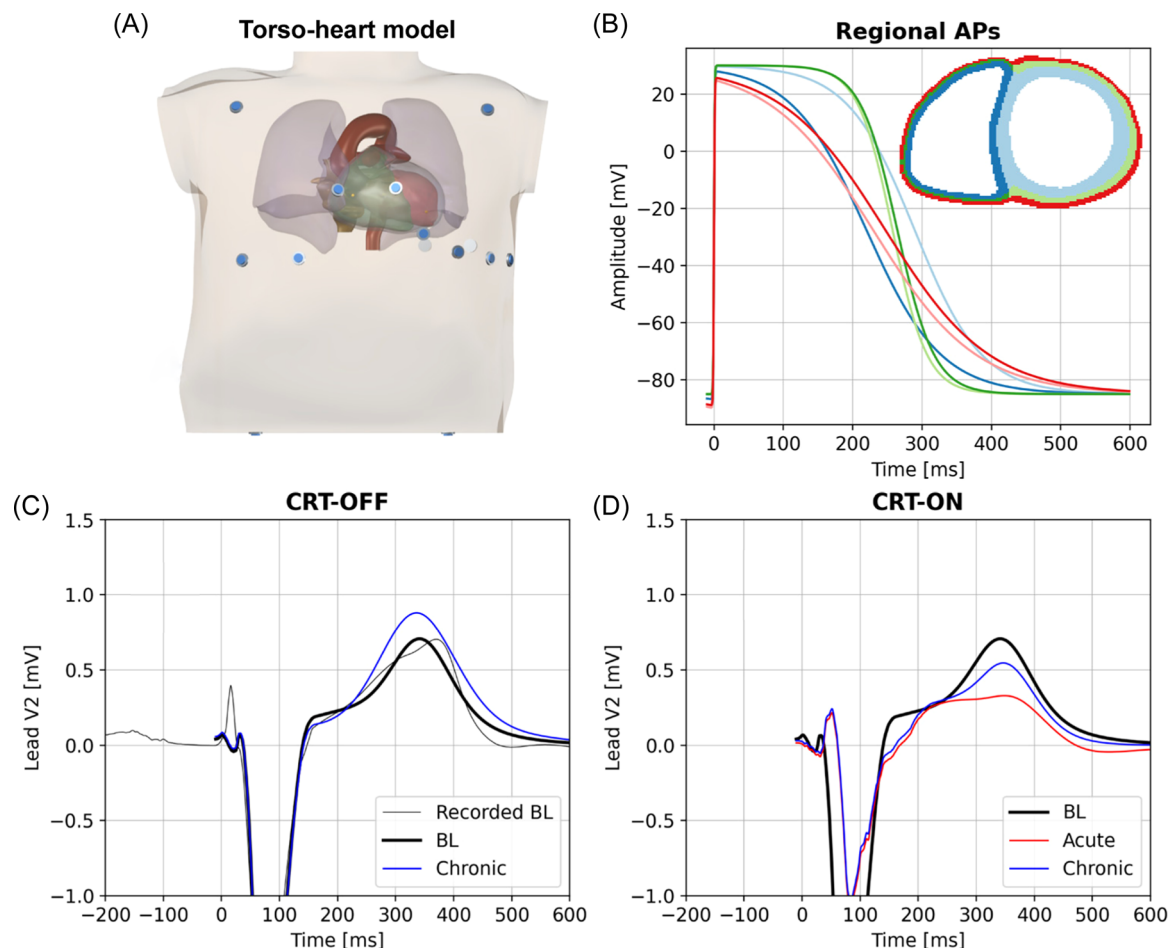
FIGURE 3 Patient-specific computer heart-torso model showing the torso with lungs, atria, ventricles, aorta, and position of the ECG electrodes (A) and shape of action potentials in the various regions of the ventricles that were required to achieve the best fit between measured and simulated baseline ECG (B). (C) Recorded (gray) and simulated ECGs at baseline and during acute and chronic CRT-OFF are displayed, and (D) presents simulated ECGs at baseline, acute and chronic CRT-ON. CRT, cardiac resynchronization therapy; ECG, electrocardiogram.

in APD between early and late activated regions have also been observed in animal hearts during longer lasting periods of ventricular pacing,[17,19,20] although one study showed APD lengthening in the very latest activated regions.[19]

Contrary to these findings Chen et al.[21] found that CRT shortened the activation recovery interval (ARI, a surrogate measure of APD) measured within ~1 cm from the LV pacing site. Also, APD measurements in isolated cells from dogs with chronic LBBB showed longer APD in late activated regions.[22] While these observations may have been affected by the experimental conditions used, also limitations in our approach should be noted. The present findings in the patient-specific computer model were obtained using T-wave area measurements, which provide an integral measurement of ventricular repolarization. A match between measured and modeled T area during chronic CRT-OFF could only be achieved by the use of an inverse relation between AT and APD for all ventricular elements. However, this first order approximation does not exclude regional differences in this relation, such as between base and apex as well as transmurally. Moreover, APD shape was kept the same between baseline and the chronic CRT conditions.

A recent study by Elliot et al. used ECG imaging to determine ventricular repolarization and ARIs in 11 patients following CRT. This study focused on ARI dispersion, which these investigators showed to be increased following CRT.[23] This finding is concordant with our results from the modeling study (Figure 4B), which showed decreases in RV ARI and increases in LV ARI. However, these authors were not able to show a reduction in overall dispersion of repolarization, possibly due to the smaller study size and because ECG imaging is largely based on electrical behavior of the epicardium of the RV and LV free walla, whereas the computer model provides a true complete ventricular information, including that of the interventricular septum.

The present study does not allow speculation about the molecular mechanisms involved in the process of T-wave changes during CRT OFF. Extensive work of Dr. Rosen's group showed involvement of stretch-induced local release of angiotensin II, modulation of transcription factors and changes in IKr and ICa,L.[24] Regional differences in stretch, coinciding with abnormal activation, appear to be crucial for inducing cardiac memory. Sosunov et al.[18]
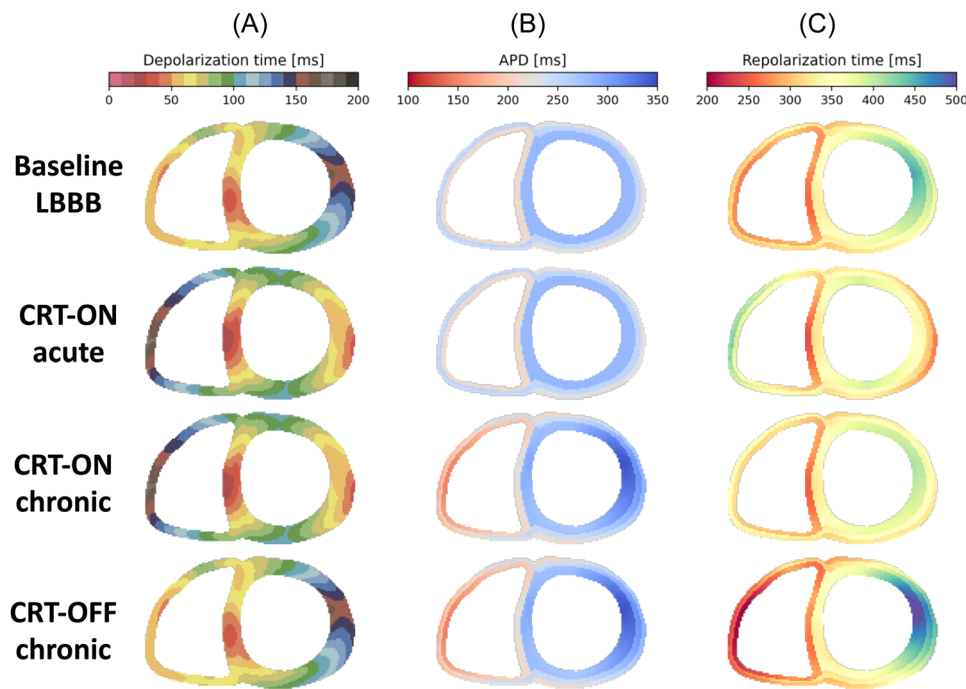
FIGURE 4 Simulations of depolarization times (A), action potential durations (APD, B) and repolarization times (C), during different situations in cardiac resynchronization therapy (CRT) (row headers). (D) The distribution of repolarization times of the right (RV, light blue) and left ventricle (LV, pink) and their dispersions (measured as interquartile range) for the indicated situation. The black arrow at the last of all repolarizations indicates the end of the T-wave. CRT, cardiac resynchronization therapy; LV, left ventricular; RV, right ventricular.
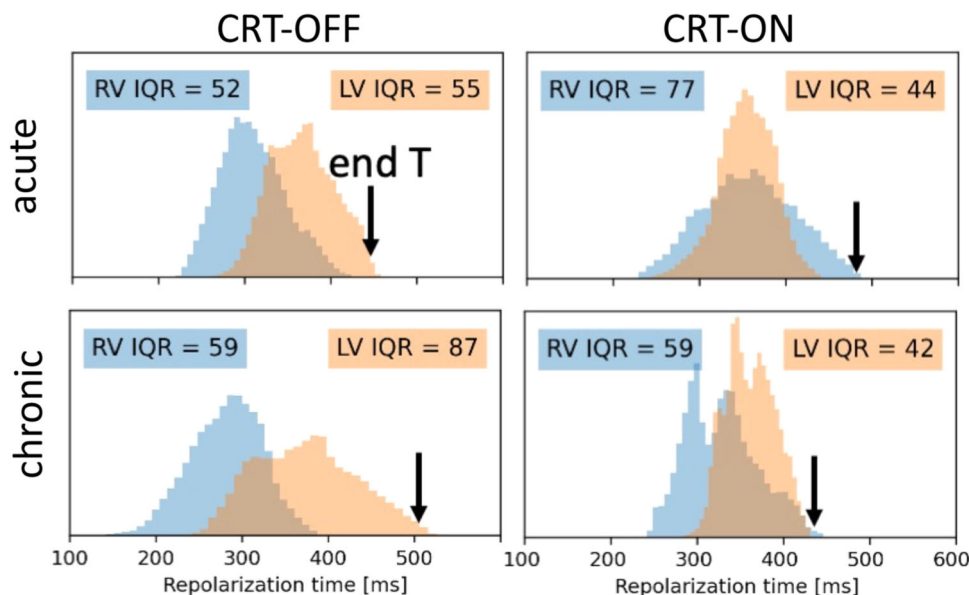

FIGURE 5 Distribution of repolarization times in the patiens-specific model during acute and chronic CRT-OFF and CRT-ON. Blue bars denote RV repolarization occurrence and pink bars LV repolarization. The black arrow indicates the moment of last repolarization and would indicate end of the T-wave. CRT, cardiac resynchronization therapy; LV, left ventricular; RV, right ventricular.

showed that mechanical unloading of the LV or blocking excitation–contraction coupling attenuated the development of cardiac memory. Based on this information Kuijpers et al.[25] proposed that T-wave memory is mediated by mechanoelectrical feedback, aiming at homogenization of myocardial work. Their computer

simulations indicated that such mechano-electrical coupling leads to a prolonged APD near the LV pacing region and lower overall dispersion of repolarization, thus in line with the results from the present study. Data from the experimental tachy-LBBB-induced dyssynchronous heart failure model showed among others, changes

in the L-type calcium channel[22] which plays an important role in regulation of both APD and contraction.

4.3 | Limitations of the study

The present work should be considered as a proof of principle study. It was performed in a relatively small group of patients from a single center, which precludes investigating the relation between the relatively rare occurrence of arrhythmia and T-wave changes in CRT patients. Other studies in a similar patient population showed an incidence of arrhythmia of 14%[4] and 20%,[26] which would have resulted in a maximum of six cases in our study. Future studies may focus on this relation, by including a brief halt of CRT at follow-up (CRT-OFF) to measure T-wave area next to device read outs.

The computer simulation was performed using data of a single patient. Future studies should include a larger number and variety of patients, including those with scar and a variation in LV pacing sites. Moreover, AP shape may be varied. Finally, physiologically based action potential models could be used to explain the electric remodeling at the level of ion channels conductivities.

5 | CONCLUSIONS

T-wave area is a sensitive marker for adaptations in ventricular repolarization that occur within a week of CRT. The T-wave changes appear explained by an inverse relation between activation and RT changes that lead to a reduction in RV and LV dispersion of repolarization during chronic CRT.

ORCID
Simone Pezzuto http://orcid.org/0000-0002-7432-0424
Frits W. Prinzen http://orcid.org/0000-0001-8917-9032

REFERENCES

1. Glikson M, Nielsen JC, Kronborg MB, et al. 2021 ESC guidelines on cardiac pacing and cardiac resynchronization therapy. *Eur Heart J.* 2021; 42: 3427–3520.
2. Medina-Ravell VA, Lankipalli RS, Yan GX, et al. Effect of epicardial or biventricular pacing to prolong QT interval and increase transmural dispersion of repolarization: does resynchronization therapy pose a risk for patients predisposed to long QT or torsade de pointes? *Circulation.* 2003;107:740-746.
3. Fish JM, Brugada J, Antzelevitch C. Potential proarrhythmic effects of biventricular pacing. Review. *J Am Coll Cardiol.* 2005;46: 2340-2347.
4. Barsheshet A, Wang PJ, Moss AJ, Solomon SD, Al-Ahmad A, McNitt S. Reverse remodeling and the risk of ventricular

tachyarrhythmias in the MADIT-CRT (Multicenter Automatic Defibrillator Implantation Trial-Cardiac Resynchronization Therapy). *J Am Coll Cardiol.* 2011;57:2416-2423.
5. Gold MR, Linde C, Abraham WT, Gardiwal A, Daubert JC. The impact of cardiac resynchronization therapy on the incidence of ventricular arrhythmias in mild heart failure. *Heart Rhythm.* 2011;8: 679-684.
6. Thijssen J, Borleffs CJW, Delgado V, et al. Implantable cardioverter-defibrillator patients who are upgraded and respond to cardiac resynchronization therapy have less ventricular arrhythmias compared with nonresponders. *J Am Coll Cardiol.* 2011;58:2282-2289.
7. Engels EB, Alshehri S, van Deursen CJ, et al. The synthesized vectorcardiogram resembles the measured vectorcardiogram in patients with dyssynchronous heart failure. *J Electrocardiol.* 2015;48:586-592.
8. Shvilkin A, Bojovic B, Vajdic B, Gussak I, Zimetbaum P, Josephson ME. Vectorcardiographic determinants of cardiac memory during normal ventricular activation and continuous ventricular pacing. *Heart Rhythm.* 2009;6:943-948.
9. Vandenberk B, Vandael E, Robyns T, et al. Which QT correction formulae to use for QT monitoring? *J Am Heart Assoc.* 2016;5:e003264.
10. van Everdingen WM, Schipper JC, Van'T Sant J, Misier KR, Meine M, Cramer MJ. Echocardiography and cardiac resynchronisation therapy, friends or foes? *Netherlands Heart J.* 2016;24:25-38.
11. Leenders GE, De Boeck BW, Teske AJ, et al. Septal rebound stretch is a strong predictor of outcome after cardiac resynchronization therapy. *J Card Fail.* 2012;18:404-412.
12. Pezzuto S, Kal'avský P, Potse M, Prinzen FW, Auricchio A, Krause R. Evaluation of a rapid anisotropic model for ECG simulation. *Front Physiol.* 2017;8:265.
13. Potse M. Scalable and accurate ECG simulation for reaction-diffusion models of the human heart. *Front Physiol.* 2018;9:370.
14. Pezzuto S, Prinzen FW, Potse M, et al. Reconstruction of three-dimensional biventricular activation based on the 12-lead electrocardiogram via patient-specific modelling. *Europace.* 2021;23:640-647.
15. Shvilkin A, Bojovic B, Vajdic B, et al. Vectorcardiographic and electrocardiographic criteria to distinguish new and old left bundle branch block. *Heart Rhythm.* 2010;7:1085-1092.
16. Rosenbaum MB, Blanco HH, Elizari MV, Lazzari JO, Davidenko JM. Electrotonic modulation of the T wave and cardiac memory. *Am J Cardiol.* 1982;50:213-222.
17. Costard-Jäckle A, Franz MR. Slow and long-lasting modulation of myocardial repolarization produced by ectopic activation in isolated rabbit hearts: evidence for cardiac "memory". *Circulation.* 1989;80: 1412-1420.
18. Sosunov EA, Anyukhovsky EP, Rosen MR. Altered ventricular stretch contributes to initiation of cardiac memory. *Heart Rhythm.* 2008;5: 106-113.
19. Jeyaraj D, Wilson LD, Zhong J, et al. Mechanoelectrical feedback as novel mechanism of cardiac electrical remodeling. *Circulation.* 2007;115:3145-3155.
20. Spragg DD, Akar FG, Helm RH, Tunin RS, Tomaselli GF, Kass DA. Abnormal conduction and repolarization in late-activated myocardium of dyssynchronously contracting hearts. *Cardiovasc Res.* 2005;67:77-86.
21. Chen Z, Hanson B, Sohal M, et al. Left ventricular epicardial electrograms show divergent changes in action potential duration in responders and nonresponders to cardiac resynchronization therapy. *Circ Arrhythm Electrophysiol.* 2013;6:265-271.
22. Aiba T, Hesketh GG, Barth AS, et al. Electrophysiological consequences of dyssynchronous heart failure and its restoration by resynchronization therapy. *Circulation.* 2009;119:1220-1230.
23. Elliott MK, Strocchi M, Mehta VS, et al. Dispersion of repolarization increases with cardiac resynchronization therapy and is associated with left ventricular reverse remodeling. *J Electrocardiol.* 2022;72: 120-127.

24. Rosen MR, Bergfeldt L. Cardiac memory: the slippery slope twixt normalcy and pathology. *Trends Cardiovasc Med.* 2015;25:687-696.

25. Kuijpers NH, Hermeling E, Lumens J, Eikelder HT, Delhaas T, Prinzen FW. Mechano-electrical coupling as framework for understanding functional remodeling during LBBB and CRT. *Am J Physiol Heart Circ Physiol.* 2014;306:H1644-H1659.

26. Itoh M, Yoshida A, Fukuzawa K, et al. Time-dependent effect of cardiac resynchronization therapy on ventricular repolarization and ventricular arrhythmias. *Europace.* 2013;15:1798-1804.